RSC Advances

PAPER

View Article Online
View Journal | View Issue

Cite this: *RSC Adv.*, 2017, **7**, 12503

Synchronous recovery of iron and electricity using a single chamber air-cathode microbial fuel cell†

Xiufen Li,*[ab] Yan Zheng,[ab] Pengfei Nie,[ab] Yueping Ren,[ab] Xinhua Wang[ab] and Yanfei Liu[c]

Received 13th December 2016
Accepted 2nd February 2017

DOI: 10.1039/c6ra28148f

rsc.li/rsc-advances

In recent years, microbial fuel cell (MFC) technology has become an attractive option for metal recovery/removal at the cathode combined with electricity generation, using organic substrates as electron donor at the anode. With no organic substrate supply, a single chamber air-cathode MFC was used to synchronously recover metal and electricity from a real stream containing high-strength metal, sulfate, strong acid and acidophilic chemoautotrophic bacteria (ACB). Instead, ferrous ions were used as electron donor which made the single chamber air-cathode MFC applicable for the (bio)leachate and mining/metallurgical stream sites possibly lacking organics. We showed that 71.8% iron was recovered, and 95.9% ferrous ions were removed from a real iron-laden stream. At the same time, 360.1 mV cell voltage was achieved with 88.1% of coulombic efficiency. In the presence of ACB microbes, the iron recovery and power density were increased by 8.6% and 29.2%, respectively, *via* promoting the anode electron transferring and preventing sulfur passivation of electrodes. Iron in the form of FeOOH (goethite) was recovered mainly at the anode *via* the ferrous oxidization to $Fe(OH)_3$. At the cathode, ferrous ions directly combined with oxygen and electrons into FeO, and further into Fe_2O_3. It was prospective at sites lack of organics to synchronously recover metals and electricity from real metal-laden streams using single chamber air-cathode MFC technology.

1. Introduction

Due to the combination of pollutant removal with electricity generation, microbial fuel cell (MFC) technology had potential to transform the conventional wastewater treatment processes from energy consumption to energy generation.[1,2] Its application also expanded to production of added-value products, such as H_2,[3] from treatment of wastewater. The (bio)leachate and mining/metallurgical streams were main contributor of heavy metals to water body environment. To remove metals from those streams, the methods generally involved in membrane separation,[4] electrowinning,[5] absorption,[6] biological transform *etc.*[7] On the other side, those streams also provided options for valuable metal recovery, which possibly made removal processes more economical and sustainable. Combined with electricity generation, MFC reactors recently became attractive option for metal recovery/removal at the cathode from metal-laden streams, using organic substrates as electron donor at the anode.[8–10]

Removal/recovery of metals from metal-laden streams was widely studied using dual or single chamber MFCs, in which metals were removed in the anaerobic or anoxic cathode chamber through cathode metal reduction, while organic substrates were used as the carbon and electron donor in the anode chamber.[11–16] Cr(VI) and V(V) were simultaneously reduced at the cathode in a double-chamber MFC.[16] With 20 mmol L^{-1} acetate as electron donor, copper removal of >99% from the $CuCl_2$ catholyte [1 g L^{-1} Cu(II)] were achieved over 6 to 7 days of MFC operation.[11] In a dual-chamber MFC, removal efficiencies of 97.8% and 94.6% were achieved for initial concentrations of 50 and 100 mg L^{-1} Au(III), respectively, over 12 h.[17] A maximum power output of 0.89 W m^{-2} was outputted for 100 mg L^{-1} Au(III). Removal of Au(III) from the catholyte was associated with deposition of metallic Au(0) on the cathode surface. The single chamber air-cathode microbial fuel cells achieved the power density of 3.6 W m^{-2}, and removed 90% Cd and 97% Zn mainly by bio-sorption and sulfide precipitation, from 200 μmol L^{-1} Cd and 400 μmol L^{-1} Zn solutions, respectively.[18] As reported above, metal was generally used as the electron acceptor at the cathode, and organics was as the electron donor at the anode. It was not always applicable for the (bio)leachate and mining/metallurgical stream sites possibly lack of organics.

[a]*Laboratory of Environmental Biotechnology, School of Environmental and Civil Engineering, Jiangnan University, Wuxi 214122, PR China. E-mail: xfli@jiangnan.edu.cn; Tel: +86 510 85326516*

[b]*Jiangsu Key Laboratory of Anaerobic Biotechnology, Wuxi 214122, PR China*

[c]*School of Chemistry and Chemical Engineering, Central South University, Changsha 410083, PR China*

† Electronic supplementary information (ESI) available. See DOI: 10.1039/c6ra28148f

In a double chamber fuel cell reactor with an anion exchange membrane, Fe^{2+} was abiotically removed from synthetic acid-mine drainage (ADM) water through oxidizing to insoluble Fe(III) [$Fe(OH)_3$], which precipitated at the bottom of the anode chamber or on the anode electrode *via* eqn (1).[19] Optimum conditions were a pH of 6.3 and a ferrous iron concentration above ~0.0036 mol L^{-1}. Further, Fe_2O_3 particle diameters ranged from 120 to 700 nm, with sizes that could be controlled by varying the conditions in the fuel cell, were harvested.[20] However, real (bio)leachate and mining/metallurgical streams contained high-strength metals and sulfate as well as acidophilic chemo-autotrophic bacteria (ACB),[21] which made the metal recovery/removal complicated. Moreover, it became unknown how the presence of sulfate and ACB microbes influenced electricity generation from those metal-laden streams.

$$Fe^{2+} + 3H_2O \rightarrow Fe(OH)_3\downarrow + 3H^+ + e^-, \quad (\Delta_f G^0 = +77.49 \text{ kJ mol}^{-1}) \qquad (1)$$

Here, we used single chamber air-cathode MFCs to recover metals combined with electricity generation from real stream contained 50.1 mmol L^{-1} Fe^{2+}, 14.1 mmol L^{-1} Fe^{3+} and 52.1 mmol L^{-1} SO_4^{2+} as well as ACB microbes. The metal precipitates were identified using scanning electron microscopy (SEM) and X-ray photoelectron spectroscopy (XPS), and metal recovery mechanism was analyzed. We showed here that, with no organic substrates as electron donor, 71.8% iron was recovered and 343.31 mW m^{-2} power density was achieved with 88.1% of coulombic efficiency. In the presence of ACB microbes, the iron recovery and power density were increased by 8.6% and 29.2%, respectively, *via* promoting the anode electron transferring and preventing sulfur passivation of electrodes. The results might be useful for the investigations that metals were recovered using MFCs, with no organics as electron donor, from (bio)leachate and mining/metallurgical streams contained high-strength metal, sulfate, strong acid and ACB microbes.

2. Materials and methods

2.1. Setups and bioleaching solution

Equipped with air-cathodes, single-chamber MFC reactors with an internal volume of 28 mL were used in this study (Fig. 1). With a normalized surface area of 7.1 cm^2 (one side), anodes were made of pretreated graphite felt (non wet-proofed, Beijing Sanye Cabon Co. Ltd., China). The cathode was prepared through applying platinum powder (0.5 mg cm^{-2} Pt, Hispec 3000, Shanghai Hesen Electric Co. Ltd., China) and four diffusion layers (polytetrafluoroethylene, PTFE) on 30 wt% water-tight carbon cloth (HCP 330P, Shanghai Hesen Electric Co. Ltd., China) as previously described.[19] Both electrodes paralleled to each other with a distance of 1.5 cm and were connected by a piece of titanium wire across an external loading of 500 Ω.

The real iron-laden stream used here was obtained by bioleaching FeS power as previously described.[22] The mixture of 10 mL effluent, from the existing well-running membrane bioreactor (MBR) treating synthetized municipal wastewater in our lab, and 90 mL anode medium [0.20 g L^{-1} $(NH_4)_2SO_4$, 3.93 g L^{-1} $K_2HPO_4 \cdot 3H_2O$, 0.50 g L^{-1} $MgSO_4 \cdot 7H_2O$, 0.19 g L^{-1} $CaCl_2$, and 10.00 g L^{-1} elemental sulfur] was adjusted to pH = 2.5 and transferred into 250 mL serum bottles. The bottles were put in a shaker of 150 rpm, and cultivated for at 30 °C. One month later, the bottles were taken out of the shaker and naturally settled. The supernatant was refreshed using the anode medium and continued to cultivate as described above. Three months later, the inocula contained ACB microbes were obtained[23] and its pH level was ~2.5. ACB microbes could grow well in strong acid solution and tolerated high-strength metals under both anaerobic and aerobic environment.[24,25] Importantly, ACB microbes had ability to take S^0 as electron donor (during which S^0 was oxidized to SO_4^{2-}) and ferric ions or electrode as electron acceptor, consequently preventing sulfur passivation of electrode.[26,27]

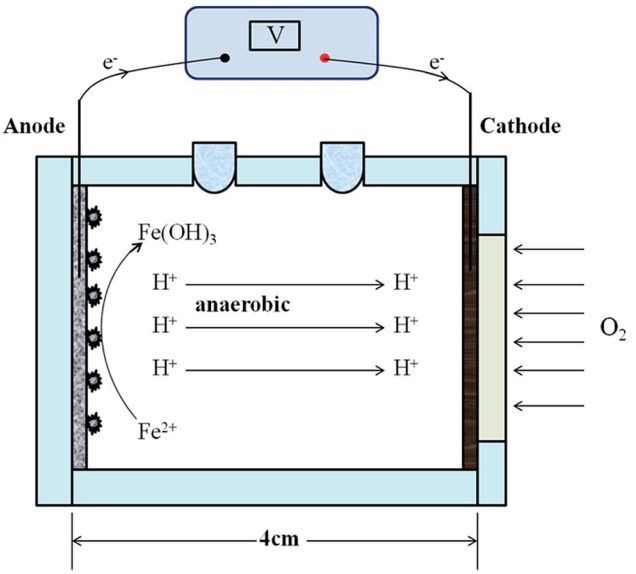

Fig. 1 Schematic diagram of single chamber air-cathode MFC reactor. It had an internal volume of 28 mL. With a normalized surface area of 7.1 cm^2, the anode paralleled to the cathode with a distance of 1.5 cm and were connected by a piece of titanium wire across an external loading of 500 Ω.

14 mL inocula in brown color was fully mixed with 25 g L^{-1} of FeS power and added to the anode chamber of a double-chamber MFC reactor separated by proton exchange membrane (Nafion-117, DuPont Company, USA), followed by addition of anode medium to 28 mL. Then, 28 mL phosphate buffer solution (PBS, 11.53 g L^{-1} $Na_2HPO_4 \cdot 12H_2O$, 2.77 g L^{-1} $NaH_2PO_4 \cdot 2H_2O$, 0.31 g L^{-1} NH_4Cl, and 0.13 g L^{-1} KCl) transferred to the cathode chamber (28 mL). Both anode and cathode were made of pretreated graphite felt, and connected by a piece of titanium wire across an external loading of 500 Ω. After the double-chamber MFC reactor above reached stable, the anode supernatant (here called real iron-laden stream and used in this study) was collected which contained 50.1 mmol L^{-1} Fe^{2+}, 14.1 mmol L^{-1} Fe^{3+} and 52.1 mmol L^{-1} SO_4^{2+} as well as ACB microbes. The pH value of real iron-laden stream was around 3.5.

2.2. Operational

For determination of the initial pH influence on electricity generation, three single-chamber MFC reactors were filled with

28 mL synthetic stream containing 50 mmol L^{-1} Fe^{2+} in an anaerobic glove box, and then the pH adjusted to 2.5 (MFC-2.5), 4.5 (MFC-4.5) and 6.5 (MFC-6.5) using 0.1 mol L^{-1} HCl and 0.1 mol L^{-1} NaOH solution, respectively. For the treatment of real iron-laden stream, the reactor (inoculated MFC) were filled with 28 mL real stream in an anaerobic glove box, and then the pH level adjusted to the optimal value determined above from 3.5. In order to investigate the role of ACB microbes carried by real iron-laden stream, another reactor (Sterile control) was filled after filtrating by 0.2 μm acetate fiber microfiltration membrane to remove ACB microbes from real iron-laden stream. All reactors were placed in a temperature-controlled room (30 °C).

The medium in the reactors was refilled when the cell voltage dropped below 20 mV. At the end of experiment, the precipitates at the bottom of reactors and on electrode surface were removed with a plastic plate and analyzed as follows. The solution was monitored for total iron and ferrous ions. The anode and cathode were softly washed using deionized water and air-dried at room temperature for the use of SEM (TM3030, HITACHI, Japan) observation. The precipitates were washed using deionized water and centrifuged three times at 3000*g*, and air-dried at room temperature for the use of XPS (AXIS HIS 165 spectrometer, Kratos Analytical) survey.

2.3. Analysis

The cell voltage (V) across the external loading (R) was automatically recorded by a computer-based data acquisition system (DAQ-2204, Taiwan ADLINK Ltd., China) at a pre-determined sampling frequency (1 h). The power output (P), normalized by the projected surface area of the anode (A), was calculated by the equation $P = V^2 (R^{-1} \times A)$. After the reactors reached stable, cyclic voltammetry (CV) scanning of the anode was conducted using an electrochemical workstation (CHI600D, CH Instruments Inc., China) in depleted substrate condition. Before analysis, the reactors were left in open-circuit for 1 h to reach the static state. The working and counter terminals of the electrochemical instrument were connected *in situ* to the anode and cathode of the examined MFC reactor, while a saturated calomel electrode (SCE, +0.242 V *vs.* the standard hydrogen electrode [SHE], Gaoshirilian Ltd., China) as the reference electrode was placed close to the anode. Prior to use, SCE was carefully rinsed with deionized water. According to the working potential of the electrodes investigated here, CV was performed from −0.9 V to +0.9 V *vs.* SCE at a scan rate of 1 mV s^{-1}.

The concentrations of total iron were quantified at 248 nm by the flame atomic absorption spectrophotometry (AA-7000, SHIMADZU, Japan) equipped with a hollow cathode lamp (GL, SHIMADZU, Japan), and ferrous ions was by phenanthroline spectrophotometric method.[28] If not analyzed immediately, the filtered samples were kept pH < 2.5 in closed vials to prevent the oxidization of ferrous to ferric ions or precipitation. At the end of experiment, the anode and cathode of the inoculated MFC reactor after dried were imaged using SEM.[29] The precipitates of both anode and cathode of the inoculated MFC reactor were respectively recorded by XPS spectrometer equipped with a monochromatized Al Ka X-ray source (1486.71 eV photons).

3. Results and discussion

3.1. Influence of initial pH on electricity generation from synthetic stream

Due to the strong dependence of eqn (1) on solution pH, the outputted cell voltages and power densities were firstly shown in Fig. 2 and 3 as varying initial pH of synthetic stream from 2.5 to 4.5 and 6.5. The peak cell voltages of three single chamber air-cathode MFC reactors firstly experienced a rapid decline and then reached a platform, suggesting that electricity heavily depended on chemical reaction. The peak cell voltages of MFC-2.5, MFC-4.5 and MFC-6.5 reactors presented to be 267.4, 352.4 and 189.6 mV. Accordingly, the power density along with initial

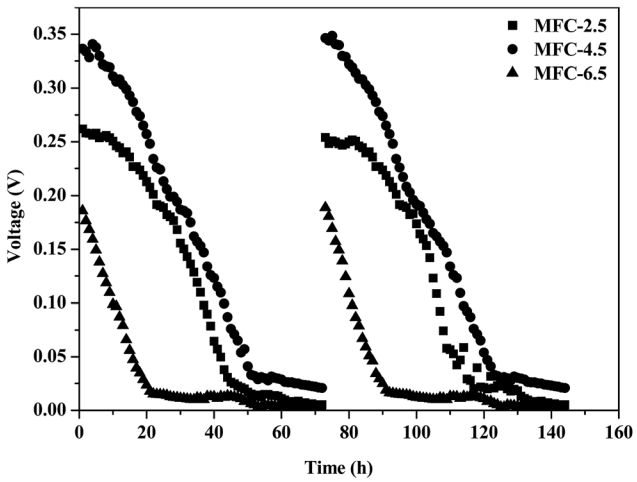

Fig. 2 Cell voltages generated from synthetic stream with 50 mmol L^{-1} Fe^{2+}. Three reactors were filled with 28 mL synthetic stream in an anaerobic glove box, and then the pH adjusted to 2.5 (MFC-2.5), 4.5 (MFC-4.5) and 6.5 (MFC-6.5) using 0.1 mol L^{-1} HCl and 0.1 mol L^{-1} NaOH solution, respectively.

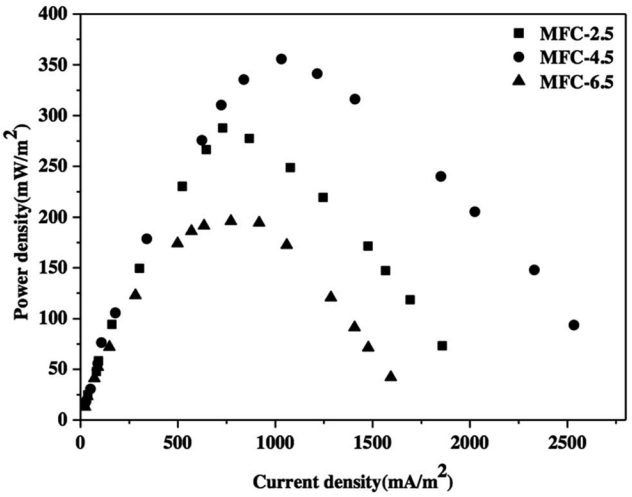

Fig. 3 Power density generated from synthetic stream. After the reactors were in open circuit for overnight, the power density curves were obtained by changing the external resistance in the range of 100 Ω to 100 kΩ.

pH variation was 139.5 mW m^{-2} for MFC-2.5, 298.9 mW m^{-2} for MFC-4.5 and 47.3 mW m^{-2} for MFC-6.5, which was negatively associated with the internal resistances (Fig. 3). The single chamber air-cathode MFC reactor with pH = 4.5 outperformed in electricity generation. The power generated at pH = 4.5 here was approximate to that of a double chamber fuel cell reactor with an anion exchange membrane treating synthetic ADM water at pH = 6.3, in which the maximum power density was 290 mW m^{-2}.[19] In the air-cathode MFC reactor, the cathode pH was always approximate to that of the anode, and the lower pH level supplied enough H^+ for the cathode reduction reaction. The shift of optimal pH from 6.3 of dual-chamber MFC to 4.5 here was possibly associated with the reactor structure, which could reduce the dosage of alkali.

At 25 °C, the solubility product constant of $Fe(OH)_2$ in aqueous solution was 8×10^{-16}.[30] Generally, when the iron ion concentration in aqueous solution was below 10^{-4} mol L^{-1}, iron hydroxide [$Fe(OH)_2$] were regarded to completely precipitate *via* eqn (2). Accordingly, [OH^-] were calculated to be around $10^{-6.5}$ mol L^{-1}, indicating that the pH level higher than 7.5 was favorable for the precipitation of $Fe(OH)_2$. The higher the pH, the more the iron hydroxide precipitates. In our single chamber air-cathode MFC reactors, the initial pH was 2.5, 4.5 and 6.5 and lowered to 2.0, 4.0 and 6.0 at the end of each reaction cycle, suggesting that ferrous iron would not precipitate in the form of $Fe(OH)_2$ *via* eqn (2). However, with the anode catalysis and electron transferring, ferrous ion easily deposited in the form of $Fe(OH)_3$ *via* eqn (1) at the anode although this reaction was thermodynamically unfavorable with $\Delta_f G^0 = +77.49$ kJ mol^{-1} under standard conditions ([H^+] = 1 mol L^{-1}, pH = 0). Synchronously, oxygen was combined with H^+ (from streams or diffused from the anode) and electrons (transferred from the external circuit) into water at the cathode. Eqn (1) was strongly pH dependent, and increasing pH made it more favorable. When the initial pH in air-cathode MFC reactors increased to 4.5 from 2.5, $Fe(OH)_3$ was more favorable to deposit with the oxidization of ferrous ions. The outputted cell voltages in MFC-4.5 reactor amounted to 352.4 mV (Fig. 2). Also, at pH = 2.5, it was difficult for $Fe(OH)_3$ to precipitate and recover iron, which further blocked the oxidization of ferrous to ferric ions, causing that the outputted cell voltage of MFC-2.5 was lower than that of MFC-4.5 reactor. The peak cell voltage of MFC-6.5 heavily turned down to 189.6 mV from 352.4 mV of MFC-4.5. Although not well understood, it was possibly associated with [H^+] decrease at pH = 6.5, which made cathode oxygen reduction lowered, consequently decreasing the outputted cell voltage.

$$Fe^{2+} + 2H_2O \rightarrow Fe(OH)_2\downarrow + 2H^+, (\Delta_f G^0 = +57.95 \text{ kJ mol}^{-1}) \quad (2)$$

3.2. Electricity generation and iron recovery from real iron-laden stream

As revealed above, the single chamber air-cathode MFC reactor at pH = 4.5 achieved the highest cell voltage when treating synthetic stream with 50 mmol L^{-1} Fe^{2+}. We replaced synthetic stream using real iron-laden stream containing 50.1 mmol L^{-1} Fe^{2+}, 14.1 mmol L^{-1} Fe^{3+} and 52.1 mmol L^{-1} SO_4^{2+} as well as ACB microbes. It showed that the peak cell voltage was 360.1 mV for the inoculated MFC reactor and 314.6 mV for the Sterile control (Fig. 4). Accordingly, the power densities were 343.31 mW m^{-2} for the inoculated MFC reactor and 265.64 mW m^{-2} for the Sterile control. In the presence of ACB microbes, the power density was increased by 29.2%. A couple of redox peaks with the potentials of about −0.1 V and +0.1 V, which was in agreement with that of biofilm,[27] was observed in CV curve of the inoculated anode (Fig. 5). It demonstrated that the anode biofilm with redox species formed due to the presence of ACB microbes carried by real iron-laden stream, and further

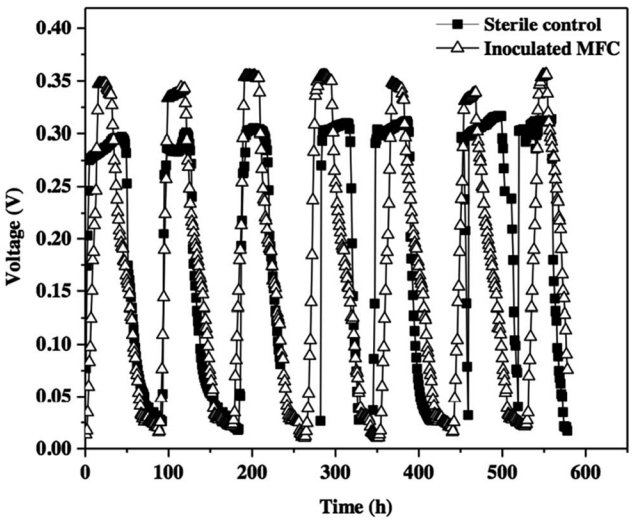

Fig. 4 Cell voltage generated from real iron-laden stream. The real stream used here was obtained by bioleaching FeS power as previously described in our lab, which contained 50.1 mmol L^{-1} Fe^{2+}, 14.1 mmol L^{-1} Fe^{3+} and 52.1 mmol L^{-1} SO_4^{2+} as well as ACB microbes. The pH value was around 3.5.

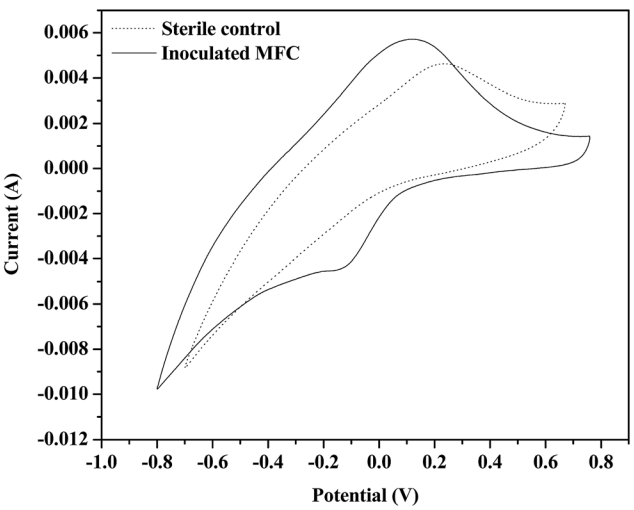

Fig. 5 CV curves of real stream system. After the reactors reached stable, CV scanning was conducted using an electrochemical workstation in depleted substrate condition. Before analysis, the reactors were left in open-circuit for 1 h to reach the static state.

promoted electrons transferring.[31] While, in CV curve of the Sterile anode, there was no redox peak, showing that it presented no electrochemical activity substances.

In single chamber air-cathode MFC reactors, SO_4^{2-} was as high as 52.1 mmol L^{-1} and could be reduced to S^0 *via* eqn (3) ($\Delta_f G^0 = -193.66$ mol L^{-1}), and S^0 deposition usually led to electrode passivation[32] and further inhibited electricity generation. Different from well-known microbes, such as sulfate-reducing bacteria,[33] ACB microbes could grow well in strong acid solution and tolerated high-strength metals under both anaerobic and aerobic environment.[24,25] Importantly, ACB microbes had ability to take S^0 as electron donor (during which S^0 was oxidized to SO_4^{2-}) and ferric ions or electrode as electron acceptor, consequently preventing eqn (3) to happen.[26,27] Therefore, the presence of ACB microbes in the inoculated MFC reactor made sulfur passivation of electrode avoidable and the outputted cell voltage was higher than that of the Sterile control. It also was higher than that of a double chamber fuel cell reactor treating synthetic ADM water with no microbes.[19]

$$SO_4^{2-} + 8H^+ + 6e^- \rightarrow S^0\downarrow + 4H_2O, (\Delta_f G^0 = -193.66 \text{ mol } L^{-1}) \quad (3)$$

At the end of experiment, the total iron ion concentration decreased to 1218.6 mg L^{-1} for the Sterile control and 1012.3 mg L^{-1} for the inoculated MFC reactor, respectively, from 3595.2 mg L^{-1} at the beginning of experiment (Table 1). The iron recovery rate was calculated to be 66.1% for the Sterile control and 71.8% for the inoculated MFC reactor by precipitating on the anode and cathode as well as at the bottom of reactors. Accordingly, the total iron precipitates collected were 184.0 mg and 196.0 mg (Table 1) and was light-brown color to the naked eyes (Fig. S1†), and the anode precipitates amounted for 83.2% and 83.7%, respectively. It showed that the iron recovery mainly completed on the anode and was dominated by eqn (1), which was in agreement with the results of Cheng *et al.*[19] In addition, the ferrous ion concentration in the inoculated MFC reactor decreased to 114.4 mg L^{-1} from 2805.6 mg L^{-1}, showing the removal rate of ferrous iron was as high as 95.9%.

With 95.9% ferrous ions removed in the inoculated MFC reactor, there was 1.35 mmol electrons released to the anode (eqn (1)). Based on the cell voltage across 500 Ω external resistance, the current generated was equivalent to 1.19 mmol electrons over one stable reaction cycle, and the coulombic efficiency of the inoculated MFC reactor was calculated to be 88.1% higher than 72% obtained using bacteria and acetate.[34] However, the ferrous removal and coulombic efficiency here were slightly lower than the literature.[19] It might be attributed to oxygen diffusion to the anode from the air cathode and the presence of unknown electron acceptors in real streams. Anyway, it demonstrated that single chamber air-cathode MFC technology had potential to synchronously recover metal and electricity from real metal-laden streams.

Table 1 Distribution of iron in the sterile control and inoculated MFC reactors at pH = 4.5 before and after operation. The reactors were filled with real stream containing 50.1 mmol L^{-1} Fe^{2+}, 14.1 mmol L^{-1} Fe^{3+} and 52.1 mmol L^{-1} SO_4^{2+} as well as ACB microbes

Items	Sterile control	Inoculated MFC reactor
Initial concentration of total iron (mg L^{-1})	3614.3	3614.3
Final concentration of total iron (mg L^{-1})	1218.6	1012.3
Anode precipitate (mg)	153	164
Cathode precipitate (mg)	19	26
Precipitate at the reactor bottom (mg)	12	6
Sum of precipitate (mg)	184	196

3.3. SEM observation and XPS analysis of precipitate and electrodes

At the end of experiment, the precipitates of the anode and cathode as well as the anode surface of the inoculated MFC reactor after air-dried were observed using SEM (Fig. 6), and the precipitates was surveyed using XPS (Fig. 7). As can be seen, the anode precipitate presented to be coarse with some bumps (Fig. 6a). The cathode precipitate grew a large amount of irregular solid pellets or flocs (Fig. 6b), suggesting that the anode precipitate was different from the cathode. Additionally, the anode surface was covered by rod-shaped bacteria (Fig. 6c), which was in agreement with the electro-active biofilm formation (Fig. 5). The anode precipitate contained O, Fe, Na, Mg, Cl and S elements as revealed by the XPS survey (Fig. 7a), and the O absorption peak was strongest followed by that of Fe element. It indicated that the anode precipitate mainly contained O and Fe elements, probably were iron oxides carrying a small amount of sodium and magnesium salts in. In XPS spectra, the absorption peak of O element appeared at the binding energy of around 531.1 eV, and O element here was attributed to iron(III) hydroxide oxide (FeOOH).[35] The absorption peak of Fe element occurred at the binding energy of around 710.1 eV, which was also attributed to iron(III) hydroxide oxide (FeOOH).[36] It concluded that the anode precipitate was dominated by iron(III) hydroxide oxide (FeOOH), which was in agreement with the result of Cheng *et al.*[20] In addition, a weak absorption peak of S element appeared at the binding energy of 169.1 eV in the XPS spectra, suggesting that there was a small amount of sulfate in the anode precipitate.[37] There was no S^0 detected in the anode precipitate according to Lindberg *et al.*,[38] which was possibly associated with ACB microbes presented in real iron-laden stream.

The XPS spectra of cathode precipitate was revealed in Fig. 7b. There were O, Fe, S, K, Na, Mg and Cl elements, which was slightly complicated than that of the anode precipitate. O and Fe elements still remained to be dominant. Different from Fe spectra of anode, the absorption peak of Fe element occurred at the binding energy of around 712.1 eV, and was regarded to be from iron(III) oxide.[39] O element was from metallic oxide because the binding energy was at around 532.1 eV.[40] It suggested that, different from the anode precipitate, the cathode precipitate mainly contained Fe_2O_3. Similarly, the S absorption peak revealed to be sulfate,[37] but not S^0.

In the cathode precipitate, because there was a certain amount of K element and the S absorption peak was heavily

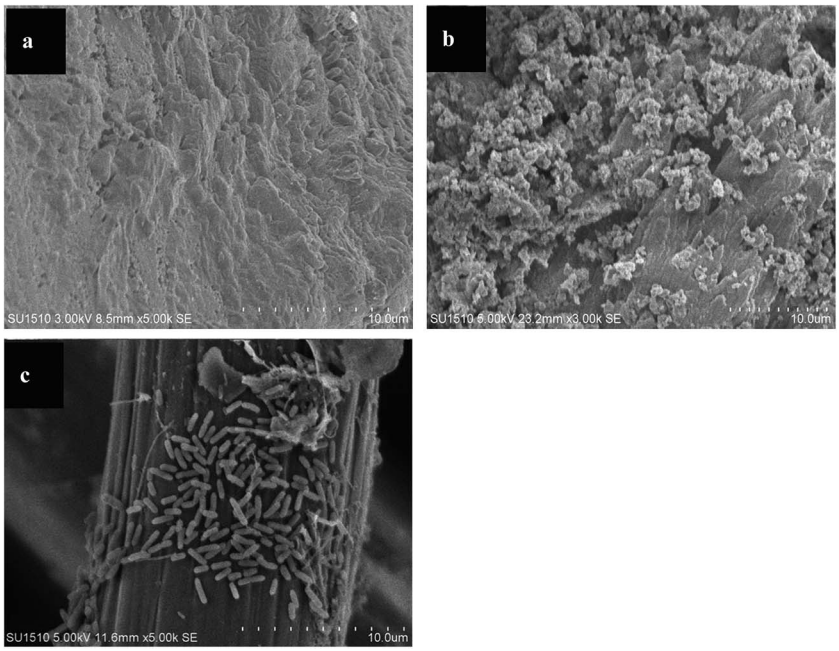

Fig. 6 SEM images of the precipitates from anode (a) and cathode (b) as well as anode surface (c) of the inoculated MFC reactor at the end of experiment.

stronger than that of the anode precipitate, we speculated that jarosite [$KFe_3(SO_4)_2(OH)_6$] precipitated *via* eqn (4) with the thermodynamic favorable free energy ($\Delta_f G^0 = -135.45$ kJ mol^{-1}). Further, the jarosite electrode passivation possibly took place.[41] However, jarosite dissolution reactions (eqn (5) and (6)) in lower pH solution were also thermodynamically favorable with the free energies of −116.50 and −93.70 kJ mol^{-1}, respectively.

$$2Fe(OH)_3 + K^+ + Fe^{3+} + 2SO_4^{2-} \rightarrow KFe_3(SO_4)_2(OH)_6\downarrow, \quad (\Delta_f G^0 = -135.45 \text{ kJ mol}^{-1}) \quad (4)$$

$$KFe_3(SO_4)_2(OH)_6 + 8H^+ + 3e^- \rightarrow K^+ + 3Fe^{2+} + 2HSO_4^- + 6H_2O, \ (\Delta_f G^0 = -116.50 \text{ kJ mol}^{-1}) \quad (5)$$

$$KFe_3(SO_4)_2(OH)_6 + 6H^+ + 3e^- \rightarrow K^+ + 3Fe^{2+} + 2SO_4^{2-} + 6H_2O, \quad (\Delta_f G^0 = -93.70 \text{ kJ mol}^{-1}) \quad (6)$$

Based on eqn (7), the reduction potential (E^0) was calculated to be +0.402 V for eqn (5) and +0.324 V for eqn (6) under standard conditions. The potential under nonstandard conditions could be given by Nernst equation. Jarosite dissolution reactions (eqn (5) and (6)) were pH dependent, and increasing pH made the reaction more unfavorable. Under our experiment conditions of pH = 4.5, $[K^+] = 0.67 \times 10^{-3}$ mol L^{-1}, $[Fe^{2+}] = 0.050$ mol L^{-1}, $[SO_4^{2-}] = 0.052$ mol L^{-1} and $T = 303$ K, the reduction potential was calculated to be −0.115 V for eqn (5) and −0.017 V for eqn (6). It meant that jarosite dissolution reactions only happened at the anode. Therefore, there was no K element detected in the anode precipitate and a weaker S absorption peak. In the inoculated MFC reactor, not only was there no sulfur passivation of electrodes, but also there was no jarosite passivation, although real iron-laden stream contained 0.052 mol L^{-1} SO_4^{2-}.

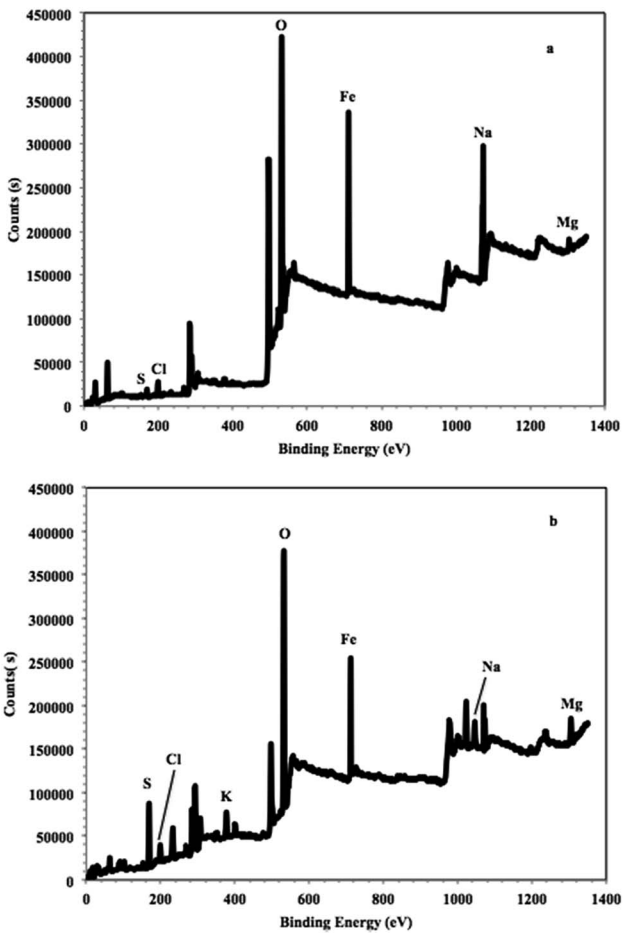

Fig. 7 XPS survey of anode (a) and cathode (b) precipitates recovered from the inoculated MFC reactor. Before analysis, precipitates were air-dried at room temperature.

Table 2 Reaction equations and their thermodynamics parameters involved in iron recovery using single chamber air-cathode MFC reactors. The free energy ($\Delta_f G^0$) was calculated based on thermodynamic data, and potentials under standard and nonstandard conditions were calculated using Nernst equation

Reaction equations	$\Delta_f G^0$ (kJ mol^{-1})	E^0 (V)	Potential equations	E' at pH = 4.5 (V)
Anode reactions				
(a) $Fe^{2+} + 3H_2O \rightarrow Fe(OH)_3\downarrow + 3H^+ + e^-$	+77.49	−0.803	$E = -0.800 + 0.006$ pH	−0.773
(b) $Fe^{2+} \rightarrow Fe^{3+} + e^-$	+74.17	−0.769	$E = -0.726$	−0.726
(c) $Fe^{2+} + 2e^- \rightarrow Fe\downarrow$	+78.87	−0.409	$E = -0.447$	−0.447
(d) $Fe^{3+} + 3e^- \rightarrow Fe\downarrow$	+4.70	−0.016	$E = -0.052$	−0.052
(e) $Fe^{3+} + 3H_2O \rightarrow Fe(OH)_3\downarrow + 3H^+$	+3.32	—	—	—
Cathode reactions				
(f) $O_2 + 4H^+ + 4e^- \rightarrow 2H_2O$	−469.08	+1.229	$E = +1.229 - 0.060$ pH	+0.959
(g) $2Fe^{2+} + O_2 + 4e^- \rightarrow 2FeO\downarrow$	−345.06	+0.894	$E = +0.846$	+0.846
(h) $Fe^{3+} + e^- \rightarrow Fe^{2+}$	−74.17	+0.769	$E = +0.736$	+0.736
(i) $4FeO + O_2 \rightarrow 2Fe_2O_3\downarrow$	−560.66	—	—	—

$$\Delta_f G^0 = -nFE^0 \quad (7)$$

3.4. Mechanism analysis of iron recovery in single chamber air-cathode MFC reactors

Based on the results and discussion above, the possible reactions associated with iron recovery in single chamber air-cathode MFC reactors treating real iron-laden stream were listed in Table 2. The reaction free energy ($\Delta_f G^0$) was calculated according to the thermodynamic data[30] and the potentials under standard conditions were obtained for the reduction and oxidization reactions *via* eqn (7).

Under our experiment conditions of pH = 4.5, $[Fe^{3+}]$ = 0.014 mol L^{-1}, $[Fe^{2+}]$ = 0.050 mol L^{-1} and T = 303 K, the ferrous oxidization to $Fe(OH)_3$ precipitate [eqn (a) in Table 2] with E' = −0.773 V was most favorable and followed by the ferrous oxidization to ferric ions [eqn (b)] with E' = −0.726 V. In the single chamber air-cathode MFC combined electricity generation with iron recovery from real iron-laden stream in this manuscript, ferrous iron, instead of organic substrates, was used as electron donor. At 25 °C, the solubility product constant of $Fe(OH)_3$ in aqueous solution was 4×10^{-38}.[30] Accordingly, $[OH^-]$ were calculated to be around $10^{-11.5}$ mol L^{-1}, indicating that the pH level higher than 2.5 was favorable for the precipitation of $Fe(OH)_3$. Therefore, the ferric ions also precipitated in the form of $Fe(OH)_3$ at pH > 2.5 [eqn (e)].

Further, $Fe(OH)_3$ was lost water to FeOOH, as demonstrated by anode XPS spectra (Fig. 7a). Additionally, the free energies ($\Delta_f G^0$) of ferrous and ferric reduction to metallic Fe(0) [eqn (c) and (d)] were +78.87 and +4.70 kJ mol^{-1} under standard conditions,[30] and the corresponding potentials (E^0) were −0.409 and −0.016 V, respectively. Compared with the potential of eqn (a) in Table 2, the formation of metallic Fe(0) was not competitive at the anode, especially at pH = 4.5 [$Fe(OH)_3$ completely precipitated]. To avoid metallic Fe(0) formation at the anode and keep sustainable electricity generation, the solution pH should be kept at higher value. From Table 2, the reduction of oxygen *via* accepting electrons transferred from the anode [eqn (f)] was most favorable at the cathode and followed by the formation of FeO [eqn (h)]. Further, the FeO oxidization to Fe_2O_3 [eqn (i)] in the presence of O_2 was also thermodynamically favorable ($\Delta_f G^0$ = −560.66 kJ mol^{-1}), and, therefore, the cathode precipitate was dominated by Fe_2O_3 (Fig. 7b). It meant that Fe_2O_3 was directly produced through ferrous oxidization using oxygen at the cathode.

Both FeOOH (goethite) and Fe_2O_3 were conductive and their precipitation on the anode or cathode would not influence the sustainable electricity generation. At the anode of single chamber air-cathode MFC reactors treating real iron-laden stream, the higher pH (>2.5) should be kept to completely precipitate $Fe(OH)_3$ and the anode product was controlled to be higher-grade FeOOH. To ensure that Fe_2O_3 dominated the cathode precipitate, enough oxygen should be supplied at the cathode.

4. Conclusions

The single chamber air-cathode MFC combined electricity generation with iron recovery from real iron-laden stream in this manuscript. Ferrous iron, instead of organic substrates, was used as electron donor, which made it applicable for the (bio)leachate and mining/metallurgical stream sites possibly lack of organics. Using the synthetic stream, the optimal initial pH of air-cathode MFC solution was determined to be 4.5 with 352.4 mV of cell voltage and 298.9 mW m^{-2} of power density. Without organic substrates as electron donor, 71.8% iron was recovered, 95.9% ferrous ions was removed and 343.31 mW m^{-2} power density were generated from real iron-laden stream at pH = 4.5. ACB microbes carried in real iron-laden stream was able to make the anode biofilm electrochemically active and further promote the electron transferring, and prevent sulfur passivation of electrodes *via* inhibiting sulfate reduction to S^0. Ferrous ions were mainly oxidized to $Fe(OH)_3$ at the anode and recovered by FeOOH. In the presence of oxygen, ferrous ions directly combined with oxygen and electrons into FeO, and further into Fe_2O_3 at the cathode. After optimization of system, it was prospective to recover metals and electricity from real streams, which contained high-strength metal, sulfate, strong

acid and ACB microbes, using single chamber air-cathode MFC technology.

Acknowledgements

This work was supported by a grant from the Research and Innovation Project for Postgraduates of Higher Education Institutions of Jiangsu Province (No. KYLX14_1159, KYLX16_0812 and SJZZ16_0216).

References

1 Y. Asensio, C. M. Fernandez-Marchante, J. Lobato, P. Cañizares and M. A. Rodrigo, *Water Res.*, 2016, **99**, 16–23.
2 C. H. Feng, L. Q. Huang, H. Yu, X. Y. Yi and C. H. Wei, *Water Res.*, 2015, **76**, 160–170.
3 N. Montpart, L. Rago, J. A. Baeza and A. Guisasola, *Water Res.*, 2015, **68**, 601–615.
4 J. Llanos, P. M. Williams, S. Cheng, D. Rogers, C. Wright, Á. Pérez and P. Cañizares, *Water Res.*, 2010, **44**, 3522–3530.
5 R. M. Ruan, X. Y. Liu, G. Zou, J. H. Chen, J. K. Wen and D. Z. Wang, *Hydrometallurgy*, 2011, **108**, 130–135.
6 G. Lofrano, M. Carotenuto, G. Libralato, R. F. Domingos, A. Markus, L. Dini, R. K. Gautam, D. Baldantoni, M. Rossi, S. K. Sharma, M. C. Chattopadhyaya, M. Giugni and S. Meric, *Water Res.*, 2016, **92**, 22–37.
7 H. T. Q. Kieu, E. Müller and H. Horn, *Water Res.*, 2011, **45**, 3863–3870.
8 K. R. Fradler, I. Michie, R. M. Dinsdale, A. J. Guwy and G. C. Premier, *Water Res.*, 2014, **55**, 115–125.
9 Y. V. Nancharaiah, S. Venkata Mohan and P. N. L. Lens, *Bioresour. Technol.*, 2015, **195**, 102–114.
10 H. M. Wang and Z. J. Ren, *Water Res.*, 2014, **66**, 219–232.
11 A. ter Heijne, F. Liu, R. V. Weijden, J. Weijma, C. J. Buisman and H. V. Hamelers, *Environ. Sci. Technol.*, 2010, **44**, 4376–4381.
12 L. Huang, J. Chen, X. Quan and F. Yang, *Bioprocess Biosyst. Eng.*, 2010, **33**, 937–945.
13 Y. Li, Y. Wu, S. Puranik, Y. Lei, T. Vadas and B. Li, *J. Power Sources*, 2014, **269**, 430–439.
14 H. C. Tao, M. Liang, W. Li, L. J. Zhang, J. R. Ni and W. M. Wu, *J. Hazard. Mater.*, 2011, **189**, 186–192.
15 G. Wang, L. Huang and Y. Zhang, *Biotechnol. Lett.*, 2008, **30**, 1959–1966.
16 B. Zhang, C. Feng, J. Ni, J. Zhang and W. Huang, *J. Power Sources*, 2012, **204**, 34–39.
17 C. Choi and N. Hu, *Bioresour. Technol.*, 2013, **133**, 589–598.
18 C. Abourached, T. Catal and H. Liu, *Water Res.*, 2014, **51**, 228–233.
19 S. A. Cheng, B. A. Dempsey and B. E. Logan, *Environ. Sci. Technol.*, 2007, **41**, 8149–8153.
20 S. A. Cheng, J. H. Jang, B. A. Dempsey and B. E. Logan, *Water Res.*, 2011, **45**, 303–307.
21 S. Panda, A. Akcil, N. Pradhan and H. Deveci, *Bioresour. Technol.*, 2015, **196**, 694–706.
22 P. F. Nie, X. F. Li, Y. P. Ren and X. H. Wang, *RSC Adv.*, 2015, **5**, 89062–89068.
23 G. Akinci and D. E. Guven, *Desalination*, 2011, **268**(1–3), 221–226.
24 L. G. Leduc, G. D. Ferroni and J. T. Trevors, *World J. Microbiol. Biotechnol.*, 1997, **13**(4), 453–455.
25 J. T. Pronk, K. Liem, P. Bos and J. G. Kuenen, *Appl. Environ. Microbiol.*, 1991, **57**, 2063–2068.
26 Y. M. Gong, A. Ebrahim, M. F. Adam, E. Mallory, T. Zhang, L. Derek and Z. Karsten, *Environ. Sci. Technol.*, 2012, **47**, 568–573.
27 A. ter Heijne, H. V. M. Hamelers and C. J. N. Buisman, *Environ. Sci. Technol.*, 2007, **41**(11), 4130–4134.
28 Y. D. Liu, S. H. Guo, R. L. Yu, K. Zou and G. Z. Qiu, *Curr. Microbiol.*, 2014, **68**(3), 285–292.
29 G. H. Gu, K. L. Zhao, G. Z. Qiu, Y. H. Hu and X. J. Sun, *Hydrometallurgy*, 2009, **100**(1–2), 72–75.
30 J. G. Speight, *Lange's Handbook of Chemistry*, McGraw-Hill Education, New York, 16th edn, 2005, ISBN 0071432205.
31 X. Qian, *Biochim. Biophys. Acta, Bioenerg.*, 2011, **1807**(4), 404–412.
32 T. Biegler and D. Swift, *J. Appl. Electrochem.*, 1979, **9**(5), 545–554.
33 O. J. Hao, L. Huang, J. M. Chen and R. L. Buglass, *Toxicol. Environ. Chem.*, 1994, **46**, 197–212.
34 J. R. Kim, S. Cheng, S. E. Oh and B. E. Logan, *Environ. Sci. Technol.*, 2007, **41**, 1004–1009.
35 N. S. McIntyre, D. G. Zetaruk and D. Owen, *Appl. Surf. Sci.*, 1978, **2**(1), 55–73.
36 G. C. Allen, M. T. Curtis, A. J. Hooper and P. M. J. Tucker, *J. Chem. Soc., Dalton Trans.*, 1974, **14**, 1525–1530.
37 K. Arata and M. Hino, *Appl. Catal.*, 1990, **59**, 197–204.
38 B. J. Lindberg, K. Hamrin, G. Johansson, U. Gelius, A. Fahlmann, C. Nordling and K. Siegbahn, *Phys. Scr.*, 1970, **1**(5–6), 286–298.
39 P. Mills and J. L. J. Sullivan, *J. Phys. D: Appl. Phys.*, 1983, **16**(5), 723–732.
40 M. S. Raven, *Surf. Interface Anal.*, 1979, **1**, 20–25.
41 K. Sasaki, Y. Nakamuta, T. Hirajima and O. H. Tuovinen, *Hydrometallurgy*, 2009, **95**(1–2), 153–158.

